A simple theory of the pycnocline and overturning- revisited

Anand Gnanadesikan

NOAA Geophysical Fluid Dynamics Laboratory, Princeton, New Jersey.

Agatha de Boer

School of Environmental Science, University of East Anglia, Norwich, United Kingdom.

Bryan K. Mignone

The Brookings Institution, Washington, District of Columbia.

A simple theory linking the pycnocline depth and volume transport of the thermohaline overturning to winds, eddies, and diapycnal diffusion was proposed by Gnanadesikan (Science, 283:2077-2079, 1999). The theory argued that the key processes for driving the overturning circulation are those which convert dense water to light water, rather than the reverse, and that in an ocean where vertical and horizontal diffusion coefficients are small, the dominant pathway of transformation must be the Southern Ocean. This implies control of the global overturning by Southern Ocean winds and eddies. This paper reviews some of the successes of the theory in explaining the circulation in diagnostic ocean general circulation models. It then considers the extent to which the necessary simplifications involved in deriving such a simple theory conceal some hidden effects involving changes in the geometry of the flow and density structure. We examine the impact of conflating the depth and thickness of the pycnocline, and demonstrate that these two scales, while similar in magnitude, have different dependencies on subgridscale parameterizations. Second, we show that changes in the winds and mixing can lead to different balances between the warm and cold water pathway supplying the North Atlantic, thus highlighting the neglected role of stationary eddies. Third, we consider impacts of allowing surface density and thus the location of deep water formation to vary. Finally, we demonstrate that the distribution of surface radiocarbon is inconsistent with the northern overturning being supplied by tropical upwelling.

1. INTRODUCTION

The question of how the ocean circulation is "driven" has been a vexed one for many years. In his classic "Physical Geography of the Oceans" (reprinted in 1963), Matthew Fontaine Maury fulminated against those who supposed that the ocean circulation was wind-driven, arguing that the variable winds of the Atlantic could never produce the steady Gulf Stream. Maury instead argued that the dominant mechanism for driving such currents was the heating of the tropics and cooling of polar latitudes.

The idea of a thermally-driven overturning was, however, challenged by Sandstrom (1908) who argued that in a domain where heating occurs at the same level as cooling, a large-scale circulation cannot be generated in the absence

of diffusion. While various parts of "Sandstrom's theorem" appear not to be correct, it contains a fundamental insight. When buoyancy is added at the same level at which it is removed, the vertical buoyancy flux, and hence the buoyancy work is zero (Papparella and Young, 2002; Gnanadesikan et al., 2005). Thus even insofar as the ocean overturning is affected by buoyancy forcing, some source of energy is required to provide the mechanical driving for the system- particularly over long time periods (Munk and Wunsch, 1998; Huang, 1999).

Two such sources have been proposed. One is the internal mixing driven by breaking internal waves. In a seminal paper, Bryan (1987) discussed the dynamics of an overturning whose magnitude is controlled by the vertical diffusion- which in turn is governed by the internal wave field controlled by winds and tides. Within this picture, most of the return flow associated with the overturning would occur in low latitudes, and decreasing the density gradient between the tropics and high latitude would lead to an increase in the pycnocline depth, but a decrease in the volume transport. The second possible source of energy is the work done by the wind on the surface geostrophic currents. Toggweiler and Samuels (1993,1998) suggested that changes in the winds, particularly within the Southern Ocean would result in changes in the meridional overturning circulation. Within this picture, the dominant location where water is transformed from dense to light is the Southern Ocean and changes in the density in the north would be expected to change only the pycnocline depth

Gnanadesikan (1999, henceforth G99) developed a simple theory that included closures for both of these pathways, as well as including the impact of mesoscale eddies. This paper revisits the G99 theory, discussing some of the ways in which it succeeds in describing ocean models- and some ways in which it falls short. In particular, it examines the ways in which the geometry of the circulation changes. Section 3 demonstrates that the theory can be used to fit the results of a suite of diagnostic ocean models. Section 4 examines the question of whether the pycnocline is governed by one length scale or two. Section 5 examines the extent to which changes in the subgridscale parameterization and winds change how the Atlantic is supplied with light water, highlighting the effect of stationary eddies. Section 6 discusses the role of the reduced gravity in setting the geometry and sensitivity of the solutions. Section 7 concludes the paper, revisiting the question of what forces drive the overturning.

2. THEORY AND MODELS

The basic idea behind the G99 theory is illustrated in Figure 1. Closures for the northern overturning M_n and tropical upwelling flux M_u in terms of the pycnocline depth

D , which is defined as the depth above which ~80-90% of the density anomaly is found. For purposes of this paper we will adopt the definition

$$D = 2\frac{\int_{z=-2500}^{0}(\sigma_2(z)-\sigma_2(z=2500))z\,dz}{\int_{z=-2500}^{0}(\sigma_2(z)-\sigma_2(z=2500))\,dz} \quad (1)$$

When calculated from real data for the region from 30S to 40N, D has a value of 894m. Closures to link D with the overturning fluxes may be taken as in Bryan (1987) and Park (1999) as

$$M_n = g'D^2/\varepsilon \quad (2a)$$

$$M_u = 2K_vA/D \quad (2b)$$

Where g' is the density contrast associated with the pressure gradient driving the overturning, ε is a "resistance coefficient" which embodies the effects of friction and geometry, K_v is the vertical diffusive coefficient, and A is the area of the tropical oceans. G99 added two other terms in the Southern Ocean, an Ekman upwelling term M_{ek} and an eddy-induced advection term M_{eddy}.

$$M_{ek} = \tau L_x/\rho f \quad (3a)$$

$$M_{eddy} = A_I L_x D/L_y \quad (3b)$$

Where τ is the mean wind stress at the tip of Drake Passage, L_x is length of the latitude circle, r is the density, f the Coriolis parameter, A_I the Gent-McWilliams diffusion coefficient and L_y the depth over which the pycnocline shallows in the south. Assuming a steady-state mass balance then leads to

$$g'D^2/\varepsilon + A_I L_x D/L_y = \tau L_x/\rho f + 2K_vA/D \quad (4)$$

This equation has several revealing limiting cases. If the Southern Ocean terms are set to zero, one recovers the result of Bryan (1987) that the overturning $M_n = M_u = (g'K_v)^{1/3}$. If the diffusive terms are set to zero, the overturning depends only on Southern Ocean winds and is independent of g' as long as it is sufficiently large that D is less than the depth of the ocean.

In order to illustrate and evaluate this theory, we present results from a number of models which have been presented in other work. The first set consists of a suite of 17 ocean-only simulations in a realistic geometry at a nominal

resolution of 4 degrees with 24 vertical levels, reported in Gnanadesikan et al. (2002), Mignone et al. (2006) and Mignone (2006). In these models, climatological monthly fluxes of heat and salt are applied to the surface and flux corrections are computed by restoring the surface temperature and salinities towards observations with a 30 day time scale. The wind stress, vertical diffusion coefficient in the upper water column, and lateral diffusion coefficient are varied together so as to produce similar pycnocline depths according to the theory, and separately to isolate the individual effects of each process. The parameters varied are the vertical diffusion, lateral diffusion and wind stress. Values for the vertical diffusive coefficient in the thermocline range from 0.15 cm^2/s (consistent with the measurements of Ledwell et al., 1993) to 1.2 cm^2/s. Values for the lateral diffusive coefficient A_I range from 100 m^2/s to 6000 m^2/s. The parameter settings are given in columns 2-4 of Table 1. In addition to the model physics, the abiotic carbon cycle was simulated in all of these runs including the effects of bomb radiocarbon using the Ocean Carbon Model Intercomparison Project, Version 2 protocols (Watson et al. 2003).

A second set of runs for which surface buoyancies are allowed to vary is made in an idealized two-basin configuration, following the work of De Boer et al. (2006a,b). This model consists of a coarse-resolution (4 degree) ocean model coupled to a dynamic sea ice model and an energy-moisture balance atmosphere. The ocean model topography is highly idealized, with a Pacific-Indian basin twice the size of the Atlantic basin, and a set of ridges distributed throughout the ocean basin to represent the effect of mid-ocean ridges. The vertical diffusion in this model is similar to the low-mixing values in the diagnostic suite, varying from 0.1 cm^2/s in the pycnocline to 1.2 cm^2/s at the ocean bottom and the lateral diffusion coefficient (used for both the GM eddy bolus flux and isopycnal diffusion) is set to 800 m^2/s. Surface wind stresses are given by the zonal component of the ECMWF wind stresses. In terms of the mechanical forcing, the simple coupled model is thus closest to model 7 in the diagnostic suite.

Surface buoyancy fluxes are given by a one-layer energy balance model, whose prognostic variables are temperature and mixing ratio. The temperature depends on the balance between radiation fluxes at the top and bottom of the domain, lateral diffusion, and latent heat released when precipitation is formed. The mixing ratio depends on evaporation from the ocean, precipitation and lateral diffusion. When it exceeds the temperature-dependent saturation mixing ratio, water vapor condenses. Precipitation that falls on land runs off to the nearest ocean point. De Boer et al. (2006a,b) report a large number of simulations with this configuration. We present a subset of these runs in which the wind stress in the Southern Ocean is multiplied by a fact ranging from 0-3.

3. THE G99 THEORY IN AN OCEAN-ONLY MODEL

We begin by examining how the theory predicts the behavior of the suite of ocean-only models. We identify M_n as the net northward transport of water with a potential density σ_0 less than 27.4 at a latitude of 40N and M_s as the net northward transport of water with a potential density σ_0 less than 27.4 at a latitude of 30S. D is averaged over the latitude range 30S to 40N. Columns 4-7 in Table 1 show the modeled D and M_s ,M_n, and M_u, the difference between them M_s and M_u. By examining the results, it is easy to see that the G99 theory reproduces the qualitatative sensitivity of the simulations to changes in subgridscale parameters. Increasing the Southern Ocean winds increases M_s and M_n. Increasing the A_I coefficient causes M_s to become more negative and M_n to decrease. Increasing K_v causes more upwelling in the tropics, makes M_s more negative and M_n larger.

A more quantitative comparison is given in Figure 2, where the results of the model suite are compared with the G99 theory. We begin with a result which is not highly optimized, in which A is the area of the oceans between 30S and 40N (2.0×10^{14} m^2), $L_x=2.5 \times 10^7$ m, $L_y=1.2 \times 10^6$ m, and $g'/\varepsilon=22.5$ is computed from (2a) by assuming that the observed D=894m is associated with 18Sv of overturning in the North Atlantic (as for example in Talley et al., 2003). Even without significant tuning the variation predicted by the theory is highly correlated with that in the models, accounting for 90% and up of the variation in D, M_s, M_u, and M_n. There are however, systematic differences between the theoretical and modeled results, with the predicted D showing significantly less range than the models, and the transports in general being overestimated.

It is possible to estimate the parameters in (5) from the model, individually regressing the overturning flux against D^2, the tropical upwelling flux against K_v/D and the southern upwelling flux against the Ekman flux at 50S and A_ID. When this is done, one obtains the solutions shown by the circles in Figure 2, which have a mean absolute error of 74 m for the pycnocline depth (vs. 105 for the nonoptimized model), and less than 2 Sv for each of the transports. The optimized model has a much smaller apparent area for the upwelling (1.13×10^{14} m^2) and predicts that only about half of the Ekman flux at 50S actually results in a transformation of dense water to light water at 30S. We will discuss the reasons for this in Section 5.

Taken together, the diagnostic models support the key insight of the G99 theory, namely that high diffusion, low wind and low-diffusion, high wind models can yield roughly the same overturning and pycnocline depths, but with different upwelling pathways. Moreover it appears that the model is quantitatively useful as well, predicting the magnitude of differences between models that result from changing the subgridscale parameters. For a simple

model, these are significant accomplishments. However, it is worth examining the limits of the theory as well as its successes, and we will focus on some such limits in the following sections.

4. THE SINGLE LENGTH-SCALE APPROXIMATION

One implicit assumption of the G99 theory is that there is a single length scale that describes the structure of the pycnocline- or in other words that the shape of the density gradient is self-similar across a range of parameter values. It is by no means obvious that this should be true. A number of thermocline theories, for example those of Salmon (1990) and Vallis (2000), distinguish between the *depth* at which the pycnocline is found and the *thickness* of the pycnocline at that depth. We may distinguish between these two concepts by denoting the pycnocline depth D as in (4) While the thickness of the gradient region H is described as

$$H = \frac{\left(\rho(z=0) - \rho(z=-2.5km)\right)^2}{\int_{z=-2.5km}^{0} \left(\partial\rho/\partial z\right)^2 dz} \qquad (5)$$

For an exponential profile D=H, but for other profiles (as illustrated in Figure 3) will not be the case. A linear profile (Figure 3b) will have H=1.5D, while for a parabolic profile where $\rho=\rho_0- \delta\rho(z/D_0+1)^2$, H=0.5D.

The distribution of H and D are noticeably different, both in data (Figure 4a and b) and in models (Figure 4c, d; Table 1). In particular, D has relatively little variation over the low latitudes, while H becomes very thin in the tropics. In relatively few places, however, is H much smaller than D. The average H in the data between 30S and 40N is 514m. On the face of things, this would tend to suggest that D and H are not separate scales as suggested in Salmon (1990) and Vallis (2000).

An examination of the dependence of D and H on subgridscale parameters (Table 1), however, shows that while the two are similar in terms of magnitude, they have different dependencies. For example, increasing the wind stress increases D (in agreement with the G99 theory) but not H. As seen in Figure 4c and d, it is possible to increase K_v and A_I together to maintain D, but such combinations do not maintain H. This demonstrates clearly that the shape of the thermocline is not in fact constant under different parameter settings- so that one should not expect too much from a theory that assumes geometric similarity.

It is worth examining the behavior of H when K_v is

large. High values of K_v result in noticeably higher values of H in the tropics and northern hemisphere, causing H and D to become of comparable magnitudes throughout the domain. When this is the case, increasing A_I reduces both H and D (Table 1) In contrast, when K_v is low H is insensitive to A_I.

5. CHANGES IN FLOW PATHWAYS

Another simplification in the theory is that it does not specifically distinguish between the Pacific, Atlantic and Indian Oceans. Does the theory really account for the interbasin thermohaline circulation? We can use the diagnostic model suite to examine this question as well. We focus on the light water (lighter than 27.4) transport through 8 sections,: 1. the South Pacific at 30S 2. the Indonesian throughflow 3. the South Indian at 30S 4. the Indian Sector of the Antarctic (30E to 140E at 40S- which in this model intersects the Australian continent). 5. the Atlantic Sector of the Southern Ocean at 40S (60W to 30E), 6. the flow between the Indian and Atlantic Oceans at 30E north of 40S 7. the flow in the Atlantic Ocean at 30S and 8. the flow in the Atlantic Ocean at 40N. Figure 5a shows these flows in subset of models (lines 5,12,14 and 16 in Table 1) corresponding to vertical diffusion coefficients of 0.15, 0.3, 0.6 and 1.2 cm^2/s. and Figure 5b shows a second subset (corresponding to lines 5, 13, 15 and 17) where the isopycnal diffusion coefficient is altered to match these vertical diffusion coefficients. Figure 6 does the same for the wind stress and lateral diffusion coefficients. A number of important conclusions can be drawn from these plots.

First, we notice that many of the pathways are relatively constant. All the models show a net northward flow of light water in the South Pacific, flow through the Indonesian archipelago and a net *southward* flow of light water if one adds up the Atlantic and Indian Ocean. The relative magnitude of these pathways does not change substantially if one varies only the vertical diffusion coefficient (Figure 5a). The majority of the flow in the circulations where K_v is varied enters the Atlantic from the south (the classic “cold water pathway”, not from the Indian ocean (the classic “warm water pathway”).

Second, there are substantial variations in whether the light waters in the Atlantic are fed by northward flow in the Atlantic or by flow around the Agulhas. Increasing the winds increasing the warm water pathway- actually driving the net light water flow negative in the Atlantic sector. This suggests that, at least in the coarse GCMs, the Atlantic inflow is not strictly controlled by Atlantic winds (a la Nof, 2003) so that the G99 picture is in fact reflecting a global circulation, not one limited to a single basin. Increasing the isopycnal diffusion coefficient has the reverse effect- favoring an inflow in the Atlantic Sector, and in some cases actually reversing the flow in across 30E in the

Agulhas region.

Third, none of these models show a classic “conveyor belt” as outlined by Broecker (1991) in which deep waters (in particular NADW) upwell in the Indian and Pacific Ocean, move through the Indonesian throughflow and are carried around the tip of South America into the Atlantic. The return flow of NADW in all of the models primarily passes through the Southern Ocean at some point. In the high diffusion models (Figure 5b) the bulk of the return flow upwelling in the Pacific feeds into the Antarctic Circumpolar Current and thence around South America in the cold water pathway. In the low-diffusion, high wind models, the dominant upwelling occurs in the Southern Ocean and one can then trace the path of light water from the Pacific, through the Indonesian throughflow, around the Agulhas and in to the Atlantic.

Fourth, the model suite demonstrates that isopycnal diffusion plays a very significant role in determining whether the return flow enters the Atlantic in the warm water or cold water pathway. This can be seen by comparing the compensated models (which all show relatively weak flow around the Agulhas) with the compensated models. The interplay between flow in the Agulhas, South Atlantic sector of the ACC and Indian Ocean sector of the ACC reveals that the southward flow of water associated with increasing eddy diffusion is not simply diffusive. Increasing the eddy diffusive coefficient actually increases the net northward flow of light water in the Atlantic sector of the ACC, something that makes very little sense in the context of a purely diffusive circulation.

The reason for this is that the “eddy” flow is not, in fact, purely diffusive. Hallberg and Gnanadesikan (2001) discussed the three ways in which the northward Eknman transport within Antarctic latitudes can be returned to the South. The first involves deep flow below the ridges and watermass transformation to the north and south of the ACC, i.e. the meridional overturning circulation. The second is the bolus flux associated with transient eddies. The third involves stationary eddies. Many theories of the ACC assume that the buoyancy transport associated with stationary eddies is essentially zero (for example Marshall and Radko, 2003) and observational studies such as Sun and Watts (2002) which assume a spatially and temporally uniform level of no motion appear to support this idea- predicting relatively small heat fluxes. However, this is not necessarily the case in realistic models in which the level of no motion is actually highly variable in space and time. The actual changes in the flow of warm water between the two high wind runs (lines 11 and 9 in Table 1) are examined in Figure 7. The dominant feature resulting from reducing the lateral diffusion coefficient is a change in the transport of light water within the ACC. This change is reflected in a deepening of the light water layer. The changes in the flow into the Indian and Atlantic basins rep-

resent relatively small changes in this flow, and are clearly associated with topographic features. This is one important reason that the optimized coefficients for the overturning involve a much weaker dependence on isopycnal diffusion and wind stress than would be assumed from looking at the data- stationary eddies actually play an important role as well.

6. THE ROLE OF DENSITY

One aspect of the G99 theory that has not received as much attention is the role of the surface densities in determining the solutions. Diagnostic models such as those used in sections 3-5 assume that the surface temperatures and salinities are known and essentially solve the boundary value problem of how the circulation translates these surface values into interior structure. However, this conceals a couple of strong assumptions, which probably do not hold in the real world.

The first is that the reduced gravity g' across the pycnocline is independent of the basic parameters of the model. This is not necessarily true. In a number of papers, the density in the North Atlantic responds significantly to changes in the Southern Ocean winds (Rahmsdorf and England, 1997), vertical diffusion (Mignot et al., 2006)., and isopycnal diffusion (Griesel and Maqueda, 2006). In the Southern Ocean, the problem is even more acute, as increases in the wind stress dilutes the relatively fresh Antarctic Surface Water with salty and warm Circumpolar Deep Water. Strengthening the winds in the Southern Ocean would then be expected to increase the flux of light water to the north, but also to increase the *density* of that water. Russell et al. (2006) present an analysis of how this works in a realistic coupled model.

A second aspect of fixing the surface density field is that it limits the formation of deep waters to the North Atlantic and fixes the location of deep water formation within this basin. Mignot et al. (2006) found that shifts in deep water formation location could be associated with changes in mixing when the boundary conditions on density. But changes in forcing can also result in changes in the dominant basin in which deep water is formed- a process that may have analogues in the paleoclimatic record (Haug et al., 1999).

This phenomenon is illustrated in Figure 8, which shows a suite of simple coupled models in which the winds are changed in the Southern Ocean. As the winds increase, the overturning in both the North Atlantic and North Pacific increases (note that the overturning here is presented in depth space rather than density space). This is consistent with the idea that more upwelling results in a greater transformation of dense water to light water which must be balanced in the north- the core insight of the G99 theory.

The details of the dependence however, are surprising.

The overturning in the Pacific increases much more strongly than in the Atlantic. Tripling the wind stress results in an increase of the Pacific overturning from 10 to 37, a more than threefold increase, while the Atlantic only rises from 24 Sv to 31 Sv. Based on the diagnostic models we would not expect such a large increase in the Pacific, as it would be expected that a deepening in the pycnocline would result in more eddy flux to the south. De Boer et al. (2006a) discuss this phenomenon in terms of the salinity balance between the deep and surface ocean. The winds in the Southern Ocean upwell water that is saltier on average than the salinity of newly formed North Pacific Deep Water. Thus an increase in upwelling will tend to make the surface ocean saltier. When the surface ocean becomes sufficiently salty the North Pacific halocline breaks down, allowing dense water to form there as well, a process which is the reverse of the classic mixed boundary condition thermohaline catastrophe (Stommel, 1961).

7. CONCLUSIONS

We have demonstrated that while the theory developed in G99 has significant skill in predicting the parameter dependence of the density structure and overturning in ocean-only models- it contains some significant oversimplifications. The biggest of these is that it effectively assumes a constant geometry of both the flow field and the density structure. In fact, this paper shows that changes in both the shape of the pycnocline in the vertical and the locations of deep water formation in the horizontal can result in behavior that is not intuitive, such as an increase in Southern Ocean winds causing switch in the dominant location of deep water formation between the Atlantic and Pacific, or a decrease in the cold water pathway. Moreover, the fact that a significant fraction of the light water exchange between the Southern Ocean and low latitudes is mediated by stationary eddies- a process not included in the G99 theory results in the failure of the theory to predict how changing isopycnal diffusion will change the light water flow in various sectors of the Southern Ocean.

Despite these caveats, however, the G99 theory still provides an intuitive picture for thinking about a number of key issues having to do with the global thermohaline circulation. First, it provides a framework for demonstrating how internal mixing may be replaced by Southern Ocean wind-driven upwelling as a driving mechanism for the global overturning. Second, it points out that the pycnocline provides a connection between the Southern Ocean and North Atlantic, and that changes in one may result in changes in the other. Third, it emphasizes the importance of the hydrological cycle, not merely in slowing down the overturning by freshening the northern latitudes, but actually maintaining it with respect to the Southern Ocean.

Finally, we return to the question of whether the global overturning is actually driven by winds or by mixing.

While both the diagnostic and prognostic model suite support the idea that the overturning can be driven by Southern Ocean winds, can they be used to say anything about whether or not it actually is driven by these winds? Two results from the diagnostic suite suggest that it is. The first has already been shown in Figure 4d where it can be seen that models with high vertical diffusion have trouble reproducing the low values of pycnocline thickness, even if they are able to reproduce the observed pycnocline depth.

An additional tracer that has been used to examine this question is radiocarbon. As discussed in Toggweiler and Samuels (1993) models with excessive upwelling in the low latitudes tend to have excessively low values of radiocarbon. Gnanadesikan et al (2004) showed that this was true for a subset of the models used here (lines 5,9, 15, and 16 in Table 1). The new model suite gives us an opportunity to extend this result. Figure 9 shows a plot of the mean tropical and Southern Ocean surface radiocarbon plotted against the ratio of tropical upwelling to northern hemisphere overturning. When this ratio is high, the overturning is driven by mixing, when it is low, it is driven by Southern Ocean winds. The observed values from the WOCE survey (Key et al., 2004 corrected to a date of 1990 by adding 20 per mille to match the models). The data shows relatively high values in the tropics and very low values in the Southern Ocean. As the models enter regimes where a substantial fraction of the northern hemisphere overturning is supplied by deep upwelling, none of the models are able to capture either the observed values or the difference between the tropics and high latitudes. Thus, while it is possible to match the observed pycnocline depth and many aspects of the flow field with high vertical and horizontal diffusion, this solution is unlikely to actually describe the real ocean.

Acknowledgments. The authors thank the Geophysical Fluid Dynamics Laboratory for support of this research, Robbie Toggweiler for many useful discussions, and Rick Slater and Joellen Russell for assistance carrying out the calculations. ADB received support from the NSF Earth System History program under grant NSF OCE-0081686 and from the Visiting Scientist Program at GFDL. BKM acknowledges support from BP/Amoco and Ford under the Princeton Carbon Mitigation Initiative.

REFERENCES

Broecker, W. S., The great ocean conveyer. *Oceanography*, 4**,** 79-89, 1991.

Bryan, F., Parameter sensitivity of primitive-equation ocean general circulation models, *J. Phys. Oceanogr.*, 17, 970-985, 1987.

De Boer, A. M., D. M. Sigman, J. R. Toggweiler, and J. L. Russell: The effect of global ocean temperature change on deep ocean ventilation. *Submitted to Paleoceanography (available at http://lgmacweb.env.uea.ac.uk/e099/).*, 2006a.

De Boer, A.M., J.R. Toggweiler and D.M. Sigman, Atlantic dominance of the meridional overturning, subm. *J. Phys. Oceanogr*., 2006b.

Gent, P., and J. C. McWilliams, Isopycnal mixing in ocean mod-

els. J. Phys. Oceanogr., 20, 150–155, 1990.

Gnanadesikan, A simple theory for the thickness of the oceanic pycnocline, *Science.*, 283, 2077-2079, 1999.

Gnanadesikan, A., R.D. Slater N. Gruber and J.L. Sarmiento, Oceanic vertical exchange and new production: A comparison between models and data , *Deep Sea Res. II* , 49:363-401, 2002.

Gnanadesikan, A., R.D. Slater and B.L. Samuels, Sensitivity of water mass transformation and heat transport to subgridscale parameterization in ocean general circulation models, *Geophys. Res. Lett.*, 30(18), 1967, 10.1029/2003GL018036, 2003.

Gnanadesikan, A., J.P. Dunne, R.M. Key, K. Matsumoto, J.L. Sarmiento, R.D. Slater and P.S. Swathi, Ocean ventilation and biogeochemical cycling: Understanding the physical mechanisms that produce realistic distributions of tracers and productivity, *Global Biogeochemical Cyc.*, GB4010, doi:10.1029/2003GB002097, 2004.

Gnanadesikan, A., R. D. Slater, P. S. Swathi, and G. K. Vallis, The energetics of ocean heat transport. *J. Climate*, 18(14), 2604-2616, 2005.

Griesel, A., and M.M. Maqueda, The relationship of meridional pressure gradients to North Atlantic Deep Water volume transport in an ocean general circulation model, *Climate Dyn.*, 26, 781-799, 2006.

Hallberg, R.W. and A. Gnanadesikan, An exploration of the role of transient eddies in determining the transport of a zonally reentrant current, *J. Phys. Oceanogr*., 31: 3312-3330, 2001.

Haug, G. H., D. M. Sigman, R. Tiedemann, T. F. Pedersen, and M. Sarnthein, Onset of permanent stratification in the subarctic Pacific Ocean. *Nature*, 401**,** 779-782, 1999.

Hellermann, S., and M. Rosenstein: Normal monthly wind stress over the World Ocean with error estimates. *J. Phys. Oceanogr.*, 13, 1093–1107, 1983.

Huang, R. X., Mixing and energetics of the oceanic thermohaline circulation. J. Phys. Oceanogr., 29, 727–746.1999.

Key, R.M., and coauthors, A global ocean carbon climatology: Results from GLODAP, *Global Biogeochem. Cyc.*, GB4031, doi: 10.1029/2004GB002247,2004.

Marshall, J. and T. Radko, Residual-mean solutions for the Antarctic Circumpolar Current and its associated overturning circulation, *J. Phys. Oceanogr.*, 33, 2341-2354, 2003.

Maury, M.F., The Physical Geography of the Sea and its Meteorology (ed. J. Leighly), Belknap Press, Cambridge, MA., 1963.

Mignone, B.K., Scientific and political economic constraints on the solution to the global warming problem, Ph.D. Dissertation, Princeton University, 2006.

Mignone, B.K., A. Gnanadesikan, J.L. Sarmiento and R.D. Slater, Central role of Southern Hemisphere winds and eddies in modulating the ocean uptake of anthropogenic carbon dioxide, *Geophys. Res. Letters* , 33, L01604, 2006.

Mignot, J., A. Levermann and A. Griesel, A decomposition of the Atlantic Meridional Overturning into physical components using its sensitivity to vertical diffusivity, *J. Phys. Oceanogr.*, 36, 636-650, 2006.

Munk, W. and C. Wunsch, The moon and mixing: Abyssal Recipes II, *Deep Sea Res.*, 45, 1977-2009, 1998.

Nof, D.,The Southern Ocean's grip on the northward meridional flow. *Progress in Oceanography*, 56**,** 223-247, 2003.

Paparella, F., and W. R. Young, : Horizontal convection is non-

turbulent. J. Fluid Mech., 466, 205–214, 2002.
Park, Y.-G., The stability of thermohaline circulation in a two-box model, *J. Physical Oceanogr*., 29,3101-3110, 1999.
Rahmstorf, S. and M. H. England,, Influence of Southern Hemisphere winds on North Atlantic Deep Water flow. *Journal of Physical Oceanogr*., 27**,** 2040-2054, 1997.
Russell, J.L., K. W. Dixon, A. Gnanadesikan, R.J. Stouffer and J.R. Toggweiler, Southern Ocean westerlies in a warming world: Keeping open the door to the deep ocean, in press, *J. Climate*, 2006.
Sandstrom, J.W., Dynamische versuche mit meerwasser, *Ann. Hydrogr. Marit. Meteor*., 36, 6-23, 1908.
Salmon, R., The thermocline as an internal boundary layer, *J. Mar. Res.*, 48, 437-469, 1990.
Samelson, R. M., and G. K. Vallis, Large-scale circulation with small diapycnal diffusion: The two-thermocline limit. J. Mar. Res., 55, 223–275, 1997.
Stommel, H.. Thermohaline convection with 2 stable regimes of flow, *Tellus*, 13, 224-230, 1961.
Sun C. and D.R. Watts, Heat flux carried by the Antarctic Circumpolar Current mean flow, *J. Geophys. Res.-Oceans*, 107, 3119, doi:10.1029/2001JC001187, 2002.
Talley, L.D., J.L. Reid and P.E. Robbins, Data-based meridional overturning streamfunctions for the global ocean, *J. Climate*, 16, 3213-3226, 2003.
Toggweiler, J.R. and B.L. Samuels., Is the magnitude of the deep outflow from the Southern Ocean actually governed by Southern Hemisphere winds?, *in The Global Carbon Cycle,* edited by M. Heimann, pp. 303-331, Springer-Verlag, Berlin, 1993.
Toggweiler, J. R., and B. L. Samuels, On the ocean's large scale circulation in the limit of no vertical mixing. J. Phys. Oceanogr., 28, 1832–1852, 1998.
Vallis, G.K., Large scale circulation and production of stratification: effects of wind, geometry and diffusion, *J.Phys. Oceanogr*., 30, 933-954, 2000.
Watson, A.J., J.C. Orr and coauthors, Carbon dioxide fluxes in the global ocean, in Ocean Biogeochemistry: The role of the ocean carbon cycle in climate change, M.J.R Fasham, ed. Springer-Verlag, pp. 123-144, 2003.

Agatha M. de Boer, School of Environmental Science, University of East Anglia, Norwich, NR4 7TJ, United Kingdom. a.deboer@uea.ac.uk.

Anand Gnanadesikan, NOAA Geophysical Fluid Dynamics Laboratory, PO Box 308, Princeton, NJ 08542, USA Anand.Gnanadesikan@noaa.gov.

Bryan K. Mignone, The Brookings Institution. 1775 Massachusetts Ave., NW, Washington, DC 20036, USA. bmignone@brookings.edu

	K_v	A_I	τ(50S)	D	H	M_s	M_n	M_u
1	0.15	100	1	1126	703	14.2	15.8	1.6
2	0.15	300	0.5	926	677	5.2	9.0	3.8
3	0.15	300	1	1085	711	14.5	15.3	0.8
4	0.15	1000	0.5	818	638	0.5	5.7	5.2
5	0.15	1000	1	920	671	7.1	9.5	2.4
6	0.15	1000	1.02	940	646	6.4	9.4	3.0
7	0.15	1000	1.7	1082	665	15.1	13.9	-1.2
8	0.15	1000	2.5	1202	668	23.3	22.0	-1.3
9	0.15	2000	1	827	638	3.4	6.8	3.4
10	0.15	2000	1.7	970	648	9.2	10.0	0.8
11	0.15	4000	2.5	972	624	10.5	8.7	-1.8
12	0.3	1000	1	962	756	5.3	12.3	7.0
13	0.3	1500	1	926	742	2.8	10.1	7.3
14	0.6	1000	1	1019	867	4.3	17.2	12.9
15	0.6	2000	1	911	801	-4.3	11.8	16.1
16	1.2	1000	1	1086	1036	-1.8	22.9	24.7
17	1.2	6000	1	852	799	-22.3	10.5	32.8

Table 1: Summary of the forcing and overturning in 17 diagnostic coarse-resolution models. Wind stresses at 50S are shown as a multiplier relative to the stress product of Hellermann and Rosenstein.

FIGURE CAPTIONS

Figure 1 : A schematic of the overturning circulation in the G99 model

Figure 2 : Evaluation of the G99 theory compared with a suite of diagnostic models. Nonoptimized results (+) show the G99 model with parameters estimated from data. Optimized results (o) show the G99 model with fluxes individually regressed against their functional form with respect to pycnocline depth D. (a) Pycnocline depth D. (b) NADW formation. (c) Tropical upwelling. (d) Southern Ocean upwelling

Figure 3. Schematic of three profiles and the associated values of pycnocline depth (D, eqn 2) and pycnocline thickness (H, eqn. 5) associated with them.

Figure 4: Pycnocline depth and thickness. (a) Pycnocline depth from the 1998 World Ocean Atlas. b) Pycnocline thickness for the 1998 World Ocean Atlas. c) Zonally averaged pycnocline depth compared with four “compensated” ocean-only models in which horizontal and vertical diffusion are varied together following G99. Note that the lines track each other, and the data, closely. D.) Zonally averaged pycnocline thickness for the same set of models as in c. Note that there is now more variation, with more diffusive models having a notably thicker pycnocline

Figure 5: Warm water flows across eight sections (positive is eastward/northward, negative westward/southward) for models where vertical diffusion coefficient is varied. Top panel (A) shows models where only Kv is varied. Bottom panel (B) shows models where Kv and AI are varied so as to compensate for each other (corresponding to the models shown in the bottom panels of Figure 4).

Figure 6: Warm water flows across eight sections (positive is eastward/northward, negative westward/southward) for models where wind stress is varied. Top panel (A) shows models where only wind stress is varied. Bottom panel (B) shows models where wind stress and A_I are varied so as to compensate for each other.

Figure 7: Illustration of how changing A_I changes the circulation of light water. Plots both show the depth in m of the s_0=27.4 surface in colors, and the transport of water above this surface with the vectors. Top: Model with A_I=4000 m^2/s (line 11 in Table 1). Bottom: Model with A_I=1000 m^2/s (line 9 in Table 1).

Figure 8: Response of the overturning circulation in a coupled ocean-sea ice-energy moisture balance atmosphere model to changes in Southern Ocean winds. Solid line shows the maximum overturning in the Atlantic as the winds are changed south of 30S. Dashed line shows the maximum overturning circulation in the Pacific. Note that increasing the winds causes the dominant sinking to shift from the Atlantic to the Pacific, a fundamental change in the geometry of the flow.

Figure 9: Radiocarbon contraints on upwelling pathway. Vertical axis shows surface radiocarbon concentration at a nominal date of 1990 in per mille. Horizontal axis shows the ratio between M_u and M_n, with small values consistent with the Southern Ocean upwelling pathway and large values consistent with tropical upwelling and mixing playing the dominant role. The models are most consistent with very little of the Northern upwelling being supplied through the tropics.

Figure 1 : A schematic of the overturning circulation in the G99 model.

Figure 2 : Evaluation of the G99 theory compared with a suite of diagnostic models. Nonoptimized results (+) show the G99 model with parameters estimated from data. Optimized results (o) show the G99 model with fluxes individually regressed against their functional form with respect to pycnocline depth D. (a) Pycnocline depth D. (b) NADW formation. (c) Tropical upwelling. (d) Southern Ocean upwelling

Figure 3. Schematic of three profiles and the associated values of pycnocline depth (D, eqn 2) and pycnocline thickness (H, eqn. 5) associated with them.

Figure 4: Pycnocline depth and thickness. (a) Pycnocline depth from the 1998 World Ocean Atlas. b) Pycnocline thickness for the 1998 World Ocean Atlas. c) Zonally averaged pycnocline depth compared with four “compensated” ocean-only models in which horizontal and vertical diffusion are varied together following G99. Note that the lines track each other, and the data, closely. D.) Zonally averaged pycnocline thickness for the same set of models as in c. Note that there is now more variation, with more diffusive models having a notably thicker pycnocline.

Figure 5: Warm water flows across eight sections (positive is eastward/northward, negative westward/southward) for models where vertical diffusion coefficient is varied. Top panel (A) shows models where only K_v is varied. Bottom panel (B) shows models where K_v and A_I are varied so as to compensate for each other (corresponding to the models shown in the bottom panels of Figure 4).

Figure 6: Warm water flows across eight sections (positive is eastward/northward, negative westward/southward) for models where wind stress is varied. Top panel (A) shows models where only wind stress is varied. Bottom panel (B) shows models where wind stress and A_I are varied so as to compensate for each other.

Figure 7: Illustration of how changing A_I changes the circulation of light water. Plots both show the depth in m of the σ_0=27.4 surface in colors, and the transport of water above this surface with the vectors. Top: Model with A_I=4000 m^2/s (line 11 in Table 1). Bottom: Model with A_I=1000 m^2/s (line 9 in Table 1).

Figure 8: Response of the overturning circulation in a coupled ocean-sea ice-energy moisture balance atmosphere model to changes in Southern Ocean winds. Solid line shows the maximum overturning in the Atlantic as the winds are changed south of 30S. Dashed line shows the maximum overturning circulation in the Pacific. Note that increasing the winds causes the dominant sinking to shift from the Atlantic to the Pacific, a fundamental change in the geometry of the flow.

Figure 9: Radiocarbon contraints on upwelling pathway. Vertical axis shows surface radiocarbon concentration at a nominal date of 1990 in per mille. Horizontal axis shows the ratio between M_u and M_n, with small values consistent with the Southern Ocean upwelling pathway and large values consistent with tropical upwelling and mixing playing the dominant role. The models are most consistent with very little of the Northern upwelling being supplied through the tropics.

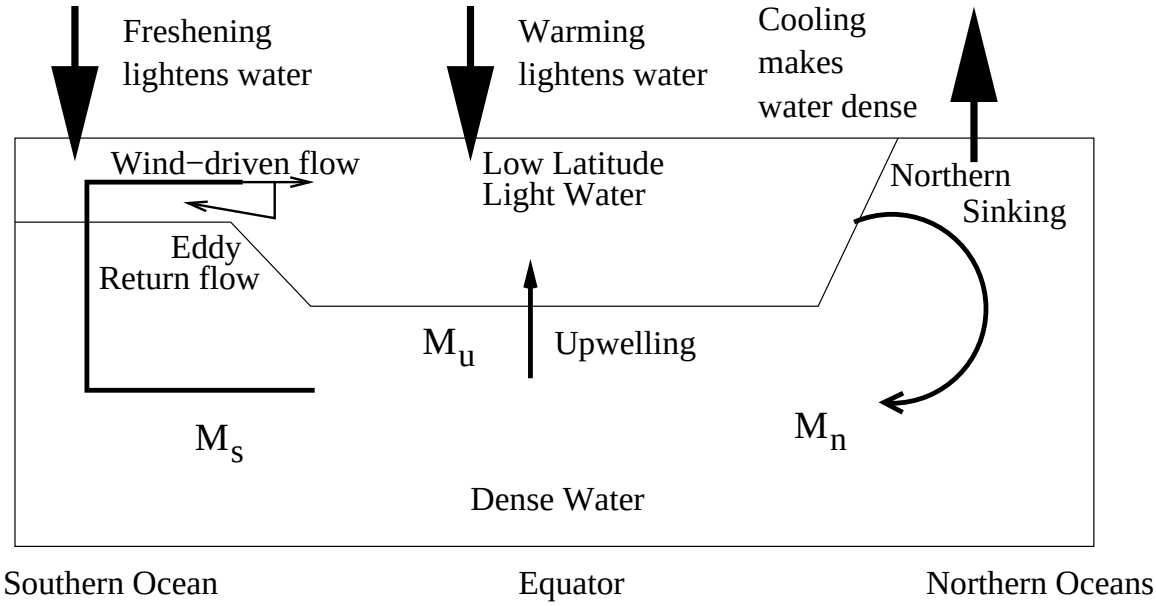

Figure 1 : A schematic of the overturning circulation in the G99 model.

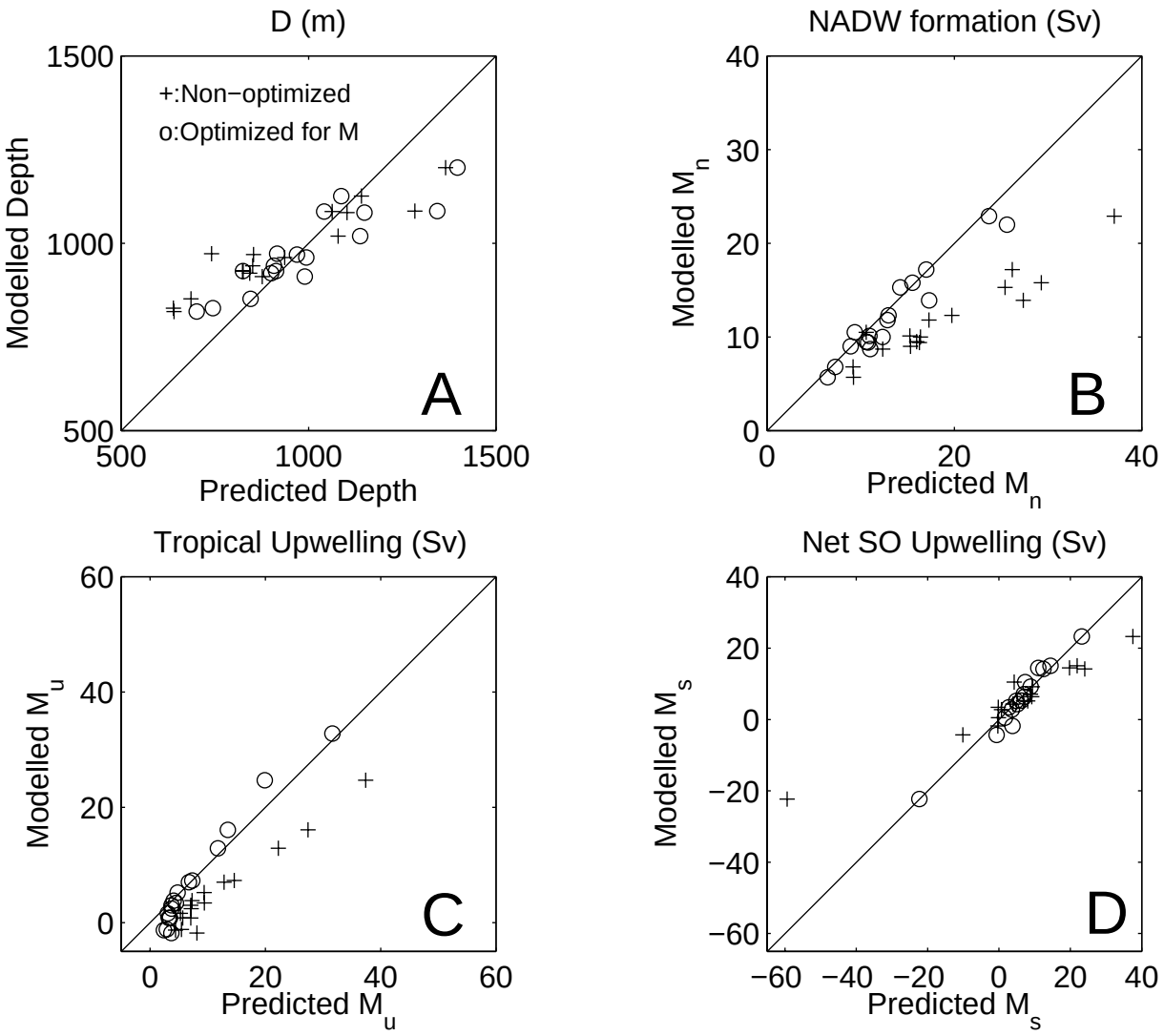

Figure 2 : Evaluation of the G99 theory compared with a suite of diagnostic models. Nonoptimized results (+) show the G99 model with parameters estimated from data. Optimized results (o) show the G99 model with fluxes individually regressed against their functional form with respect to pycnocline depth D. (a) Pycnocline depth D. (b) NADW formation. (c) Tropical upwelling. (d) Southern Ocean upwelling.

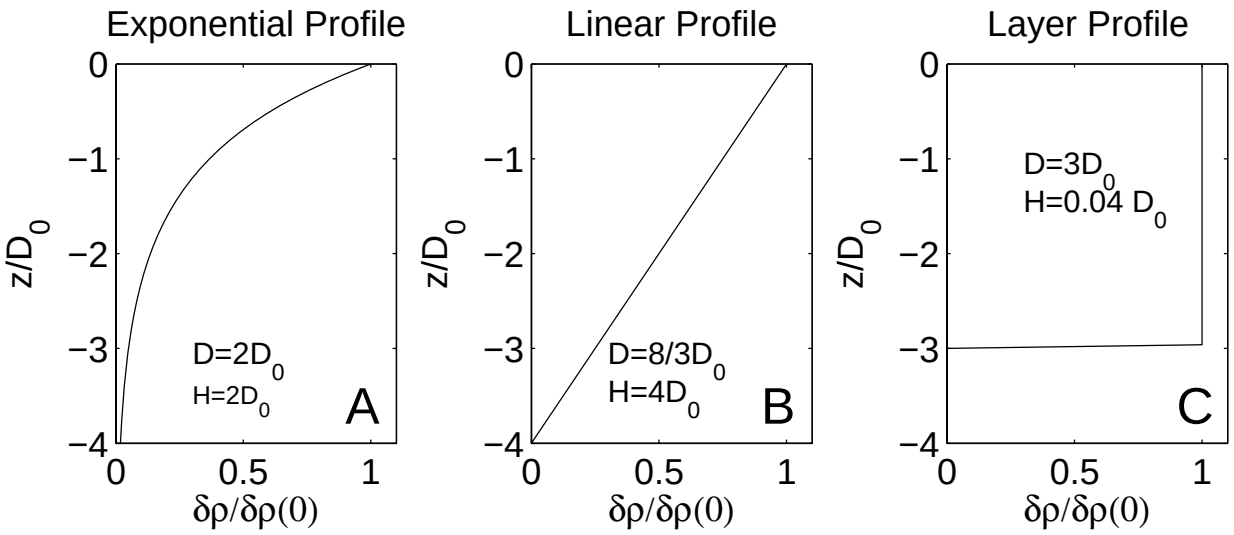

.

Figure 3. Schematic of three profiles of density anomaly normalized by the surface anomaly and the associated values of pycnocline depth (D, eqn 1) and pycnocline thickness (H, eqn. 5) associated with them.

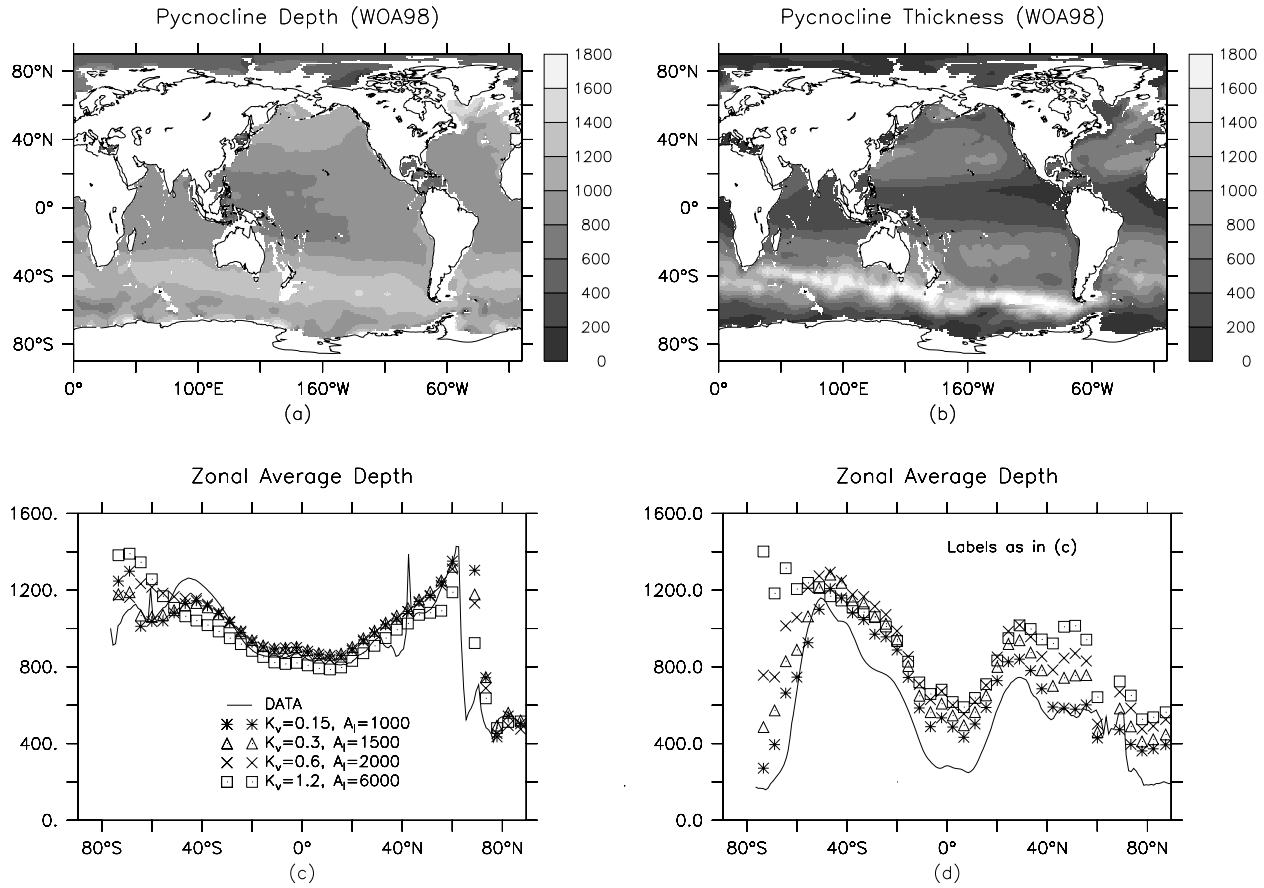

Figure 4: Pycnocline depth and thickness. (a) Pycnocline depth from the 1998 World Ocean Atlas. b) Pycnocline thickness for the 1998 World Ocean Atlas. c) Zonally averaged pycnocline depth compared with four “compensated” ocean-only models in which horizontal and vertical diffusion are varied together following G99. Note that the lines track each other, and the data, closely. D.) Zonally averaged pycnocline thickness for the same set of models as in c. Note that there is now more variation, with more diffusive models having a notably thicker pycnocline.

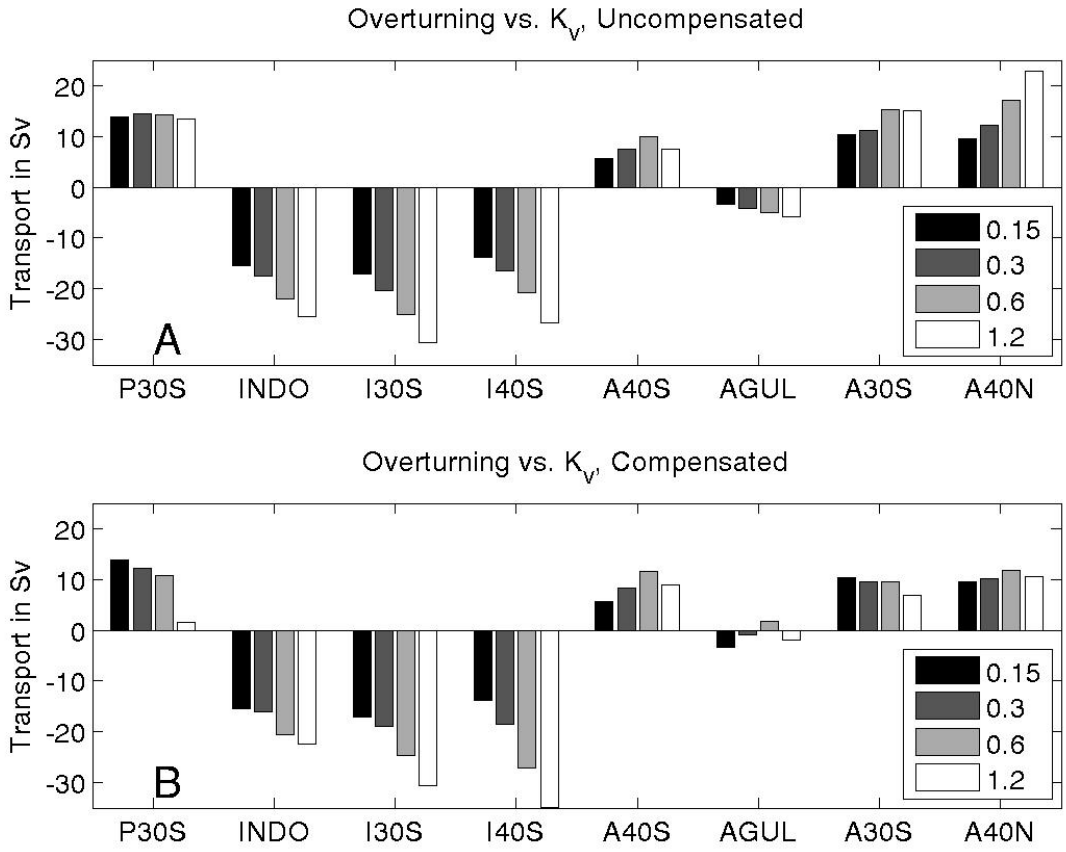

Figure 5: Warm water flows across eight sections (positive is eastward/northward, negative westward/southward) for models where vertical diffusion coefficient is varied. Top panel (A) shows models where only Kv is varied. Bottom panel (B) shows models where Kv and AI are varied so as to compensate for each other (corresponding to the models shown in the bottom panels of Figure 4).

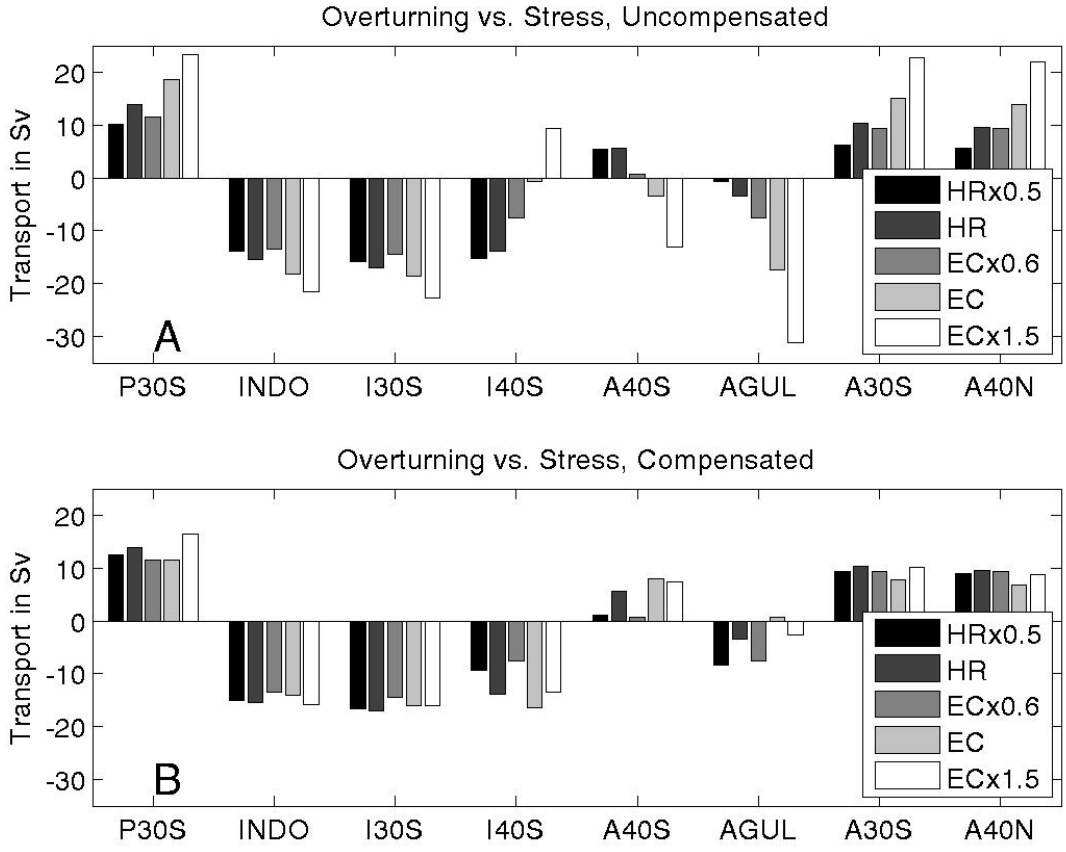

Figure 6: Warm water flows across eight sections (positive is eastward/northward, negative westward/southward) for models where wind stress is varied. Top panel (A) shows models where only wind stress is varied. Bottom panel (B) shows models where wind stress and AI are varied so as to compensate for each other.

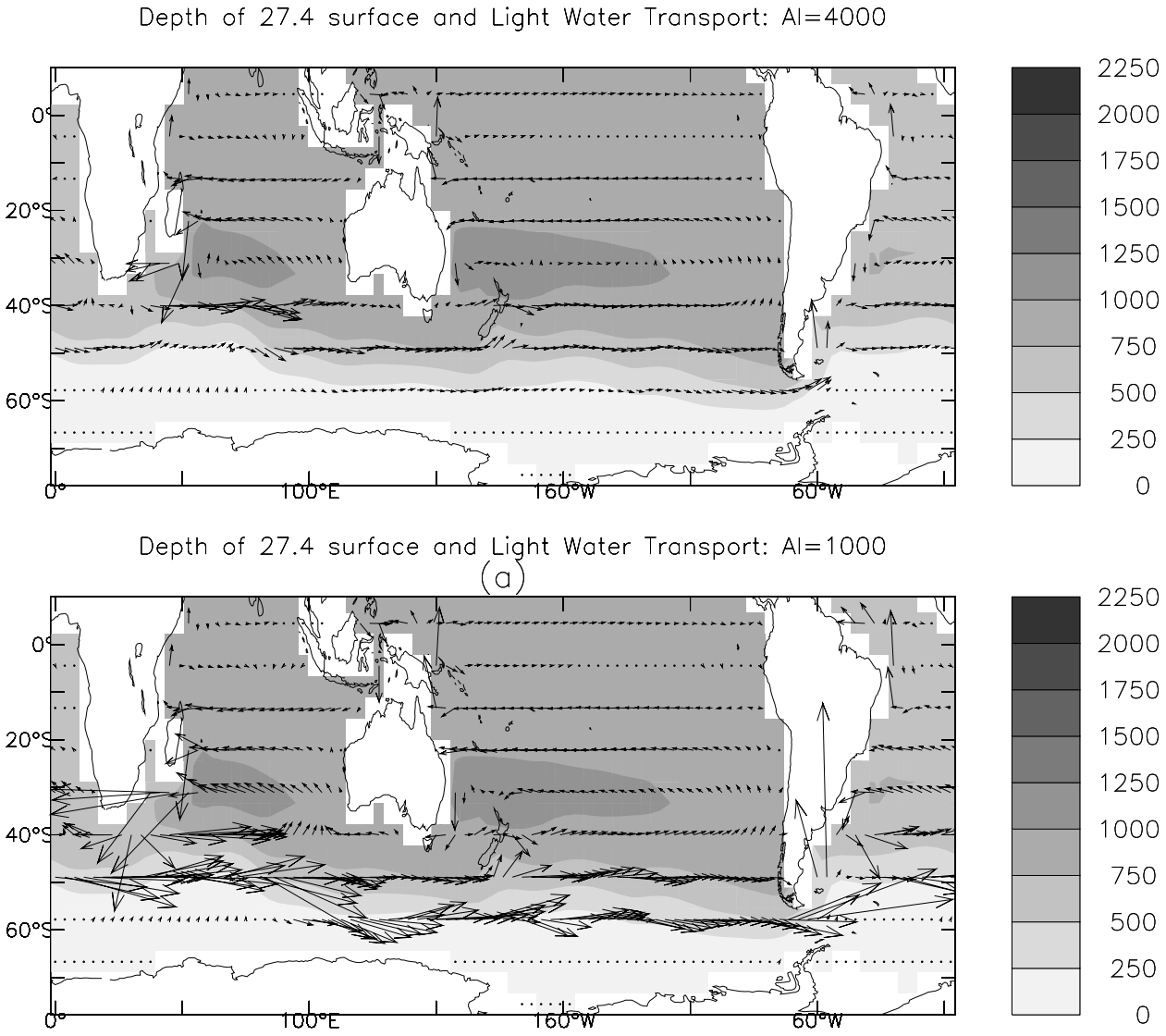

Figure 7: Illustration of how changing A_I changes the circulation of light water. Plots both show the depth in m of the σ_0=27.4 surface in colors, and the transport of water above this surface with the vectors. Top: Model with A_I=4000 m^2/s (line 11 in Table 1). Bottom: Model with A_I=1000 m^2/s (line 9 in Table 1).

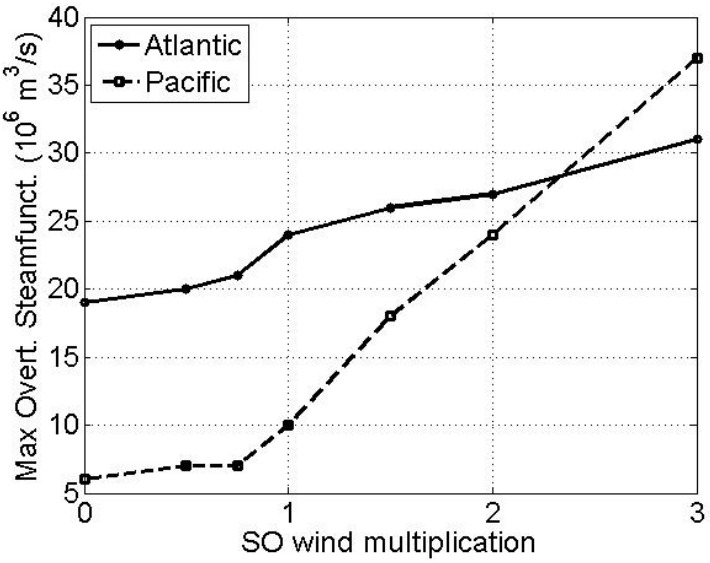

Figure 8: Response of the overturning circulation in a coupled ocean-sea ice-energy moisture balance atmosphere model to changes in Southern Ocean winds. Solid line shows the maximum overturning in the Atlantic as the winds are changed south of 30S. Dashed line shows the maximum overturning circulation in the Pacific. Note that increasing the winds causes the dominant sinking to shift from the Atlantic to the Pacific, a fundamental change in the geometry of the flow.

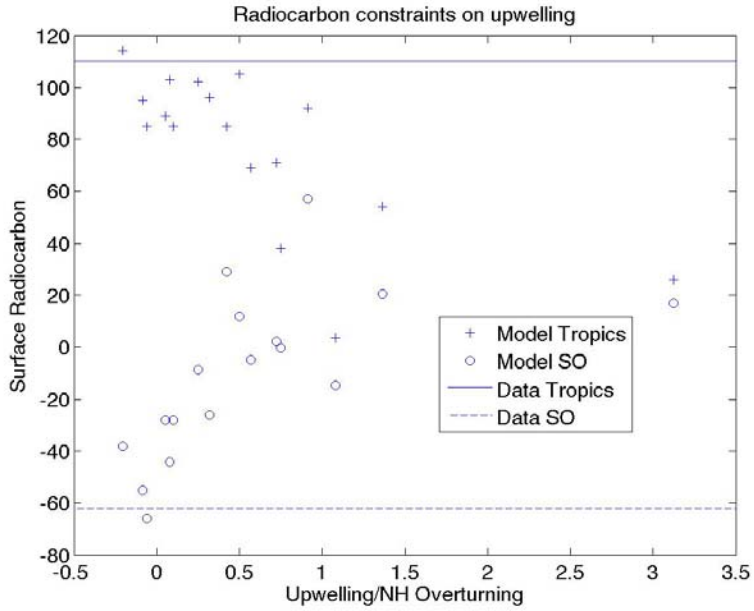

Figure 9: Radiocarbon contraints on upwelling pathway. Vertical axis shows surface radiocarbon concentration at a nominal date of 1990 in per mille. Horizontal axis shows the ratio between M_u and M_n, with small values consistent with the Southern Ocean upwelling pathway and large values consistent with tropical upwelling and mixing playing the dominant role. The models are most consistent with very little of the Northern upwelling being supplied through the tropics.